Available online at www.sciencedirect.com
ScienceDirect
Biochemical and Biophysical Research Communications 369 (2008) 100–108
BBRC
www.elsevier.com/locate/ybbrc

Structural changes of the regulatory proteins bound to the thin filaments in skeletal muscle contraction by X-ray fiber diffraction

Yasunobu Sugimoto [a,*], Yasunori Takezawa [a,1], Tatsuhito Matsuo [a], Yutaka Ueno [b], Shiho Minakata [a,2], Hidehiro Tanaka [c], Katsuzo Wakabayashi [a,*]

[a] *Division of Biophysical Engineering, Graduate School of Engineering Science, Osaka University, Toyonaka, Osaka 560-8531, Japan*
[b] *Neuroscience Research Institute, National Institute of Advanced Industrial Science and Technology, Tsukuba, Ibaraki 305-8568, Japan*
[c] *School of Nursing, Teikyo Heisei Junior College, Ichihara, Chiba 290-0158, Japan*

Received 9 November 2007
Available online 17 December 2007

Abstract

In order to clarify the structural changes related to the regulation mechanism in skeletal muscle contraction, the intensity changes of thin filament-based reflections were investigated by X-ray fiber diffraction. The time course and extent of intensity changes of the first to third order troponin (TN)-associated meridional reflections with a basic repeat of 38.4 nm were different for each of these reflections. The intensity of the first and second thin filament layer lines changed in a reciprocal manner both during initial activation and during the force generation process. The axial spacings of the TN-meridional reflections decreased by ~0.1% upon activation relative to the relaxing state and increased by ~0.24% in the force generation state, in line with that of the 2.7-nm reflection. Ca^{2+}-binding to TN triggered the shortening and a change in the helical symmetry of the thin filaments. Modeling of the structural changes using the intensities of the thin filament-based reflections suggested that the conformation of the globular core domain of TN altered upon activation, undergoing additional conformational changes at the tension plateau. The tail domain of TN moved together with tropomyosin during contraction. The results indicate that the structural changes of regulatory proteins bound to the actin filaments occur in two steps, the first in response to the Ca^{2+}-binding and the second induced by actomyosin interaction.

Keywords: Troponin; Tropomyosin; Muscle regulation; X-ray fiber diffraction; Muscle contraction; Synchrotron radiation

In vertebrate skeletal muscles, the troponin–tropomyosin complexes bound to the actin filaments, which inhibit interaction between actin and myosin in the absence of Ca^{2+} ions, undergo structural changes upon binding Ca^{2+} ions to allow actin–myosin interaction leading to muscle contraction [1]. Troponin (TN) consists of three subunits, TNI, TNC, and TNT (T1 and T2) and each subunit has an inherent function for muscle regulation [1–3]. The conformational changes of TN in solution have extensively been investigated in the presence of Ca^{2+} ions by various physicochemical methods (e.g. [2,3]) and X-ray and neutron scattering techniques [4,5]. Ca^{2+}-binding to TNC induces relatively large movements of TNI and part of TNT1 [6,7]. Recently the atomic structures of TN with and without Ca^{2+} ions were partially elucidated by X-ray crystallography, and their conformational changes upon binding Ca^{2+} ions have been discussed at atomic resolution [8,9]. In addition, the conformational changes of TN molecules in the reconstituted and/or extracted thin filaments by binding Ca^{2+} ions have been reported by neutron scattering [10,11], and those in non-overlap muscle by X-ray diffraction [12], electron microscopy (EM) [7,8],

* Corresponding authors. Fax: +81 6 6850 6515.
E-mail addresses: sugimoto@bpe.es.osaka-u.ac.jp (Y. Sugimoto), waka@bpe.es.osaka-u.ac.jp (K. Wakabayashi).
[1] Present address: Division of Chemical Engineering, Graduate School of Engineering Science, Osaka University, Toyonaka, Osaka 560-8531, Japan.
[2] Present address: ERATO Project, RIKEN Harima Institute at SPring-8, Kouto, Sayo-gun, Hyogo 679-5148, Japan.

0006-291X/$ - see front matter © 2007 Elsevier Inc. All rights reserved.
doi:10.1016/j.bbrc.2007.11.088

and fluorescence resonance energy transfer (FRET) [6,14]. However, far less is known about the structural changes of TN molecules on the thin filaments during contraction of intact muscle. There have been previous reports of the intensity changes of the limited number of the TN-associated reflections in small-angle X-ray fiber diffraction patterns have been examined and the temporal relationship between those of the other reflections and the tension development has been reported [15–17]. In this article, the intensity changes of the TN-associated meridional reflections were investigated in detail during tetanic contraction of live skeletal muscle. Structural models for conformational changes of regulatory proteins on the thin filaments due to activation and to force development are also described. This article is for the Ebashi memorial issue, in which some of the materials were taken with slight modifications from our "Regulatory Proteins of Striated Muscle" in 2006 [18].

Materials and methods

Experimental protocols. Live sartorius and semitendinosus muscles of the bullfrog (*Rana catesbeiana*) were used for the X-ray studies. They were mounted in a specimen chamber with a multi-electrode assembly. The sarcomere length of sartorius muscles was adjusted to ~2.3 μm and semitendinosus muscles were stretched beyond 4.0 μm (overstretched muscles), monitored by the optical diffraction of He–Ne laser light. The chamber was continuously perfused with chilled (10 °C) frog Ringer's solution (115 mM NaCl, 2.5 mM KCl, 1.8 m M $CaCl_2$, 0.85 mM NaH_2PO_4, 2.15 mM Na_2HPO_4 pH adjusted to 7.2). Muscles were stimulated isometrically for 1.3 s with trains of 3 ms supramaximal current pulses at 33 Hz. Each muscle was stimulated 10–15 times at resting intervals of 90 s.

The X-ray experiments using synchrotron radiation were done using the small-angle diffractometer installed at the beamline 15A1 at the Photon Factory, Tsukuba, Japan. Stimulation of live frog muscle was performed at 10 °C, and the intensity data of the TN-associated meridional reflections during an isometric contraction of muscles at full filament overlap and upon activation of overstretched muscle were measured in a time-resolved mode in the window covering the radial coordinates $0 \leqslant R \leqslant 0.015\ \mathrm{nm}^{-1}$ (R denotes the reciprocal radial coordinate from the meridian, defined by $2\sin\theta/\lambda$, where θ is the Bragg angle and λ, the wavelength of X-rays) with a CCD detector (C7300, Hamamatsu Photonics, Japan) [19]. The CCD detector was used in a sub-array mode with 64×1024 pixels and the time-resolved data were taken in an 8 ms-window followed by 7 ms for the transfer time of data so that the time between frames was 15 ms. The stimulation of muscle was synchronized to the X-ray measurement, and the tension data were simultaneously recorded. Experiments were repeated for 6–7 separate muscles and the X-ray patterns were summed. For static X-ray measurements, an image plate (an area detector, BAS-III, Fuji Film Co., Japan) [20] was used. X-ray diffraction patterns from the same muscles were recorded in the relaxing phase and at the isometric tension plateau phase for 1.0 s by opening the shutter. The measurements were repeated 10 times and the data in each phase were accumulated in the same image plate.

Intensity data. The time-resolved intensity data collected with the CCD detector were accumulated by each time frame of one muscle fiber. The meridional intensity profile was obtained by integration of the data in the range $0 \leqslant R \leqslant 0.008\ \mathrm{nm}^{-1}$. The intensities of TN-associated reflections with the basic repeat of 38.4 nm were derived by integrating their meridional profiles. The background level and the integration range were fixed in each time frame. The intensities of the first to third order of reflections were obtained from the integration of the meridional profiles.

Diffraction data collected on image plates were read out using a read-out scanner (BAS2000, Fuji Film Co., Japan) using a pixel size of 100 μm. After determining the origin and correcting the inclination angle of the image, the four quadrant patterns were folded. The intensities between the relaxing and activating patterns in pairs were normalized as described previously [21]. The intensity measurements of the TN meridional reflections were made in the radial range $0 \leqslant R \leqslant 0.001\ \mathrm{nm}^{-1}$. The intensities in the above range were summed. The intensities were also measured on the meridian in the axial direction. The TN-associated reflections partially overlapped the nearby reflections and were separated by assuming Gaussian functions. The background intensity was stripped out. The axial spacings of individual reflection profiles were estimated as their centroids [21].

Modeling. For the low-resolution modeling of the structure of TN projected onto the fiber axis, a box function model was constructed representing the globular core domain and the long tail domain, on the basis of the model from electron micrographs [22] (see Fig. 4B). Such modeling was made only for the overstretched muscle (see text). TNs bound to the thin filament were mimicked by arranging such two box functions which were staggered by 2.27 nm every 38.4 nm apart. A one-dimensional arrangement of the paired set of box functions was constructed and transformed to obtain the TN-meridional reflection intensities. By varying the parameters of the model shown in Fig. 4B, the model giving the lowest R-factor between the calculated and observed intensity data was searched.

For the high-resolution modeling, the observed thin filament-based layer line intensities were measured by the procedure described previously [21]. Firstly, using the high-angle X-ray data which are dominated by features due to F-actin, a model for F-actin was constructed by altering the actin subdomain structure. The Holmes et al.'s model [23] was used as a starting model where each of the four subdomains was divided into four subgroups. Then we incorporated tropomyosin (TM) and TN core domain + TN-T1 part into the F-actin structure and constructed a model for the whole thin filament. As the structure of TN-T1 part is unknown, it was approximated as a long helix. In the calculation, the structure of each component was defined by space-filling with small spheres with appropriate sizes and then each component moved as a rigid body. The optimum models were searched by minimizing the R-factor to obtain a reasonable fit to the observed layer line intensities in the resting and contracting states.

Results and discussion

Intensity changes of the troponin-associated meridional reflections

Fig. 1a shows a comparison of X-ray diffraction patterns in resting and contracting states of muscle at full filament overlap, and Fig. 1b a comparison of those in resting and activating states of overstretched muscle, in which the troponin-associated reflections are denoted with the letter "T" and their axial spacing in nm. Fig. 2 shows the time courses of intensity changes of the first (TN1) to the third order (TN3) troponin meridional reflections. The intensity of the TN1 reflection increased promptly at the onset of stimulation before the development of tension, and as the tension developed with $\tau_{1/2}$ ~76 ms, it decreased with $\tau_{1/2}$ ~56 ms to the level below the resting value (Fig. 2A). The magnitude of the prompt intensity increase was ca. 1.4-fold the resting value, very close to that occurring upon activation of overstretched muscle, and its time course run parallel to that of overstretched muscle. In Fig. 2B, the data are adjusted to a scale from 0 to 1, where 0 is defined as the intensity level at rest and 1 is the average intensity level between 400 and 800 ms after stimulation. In the case of TN1, the initial peak at the onset of stimulation is defined as 0. The intensity of the TN1 reflection after the

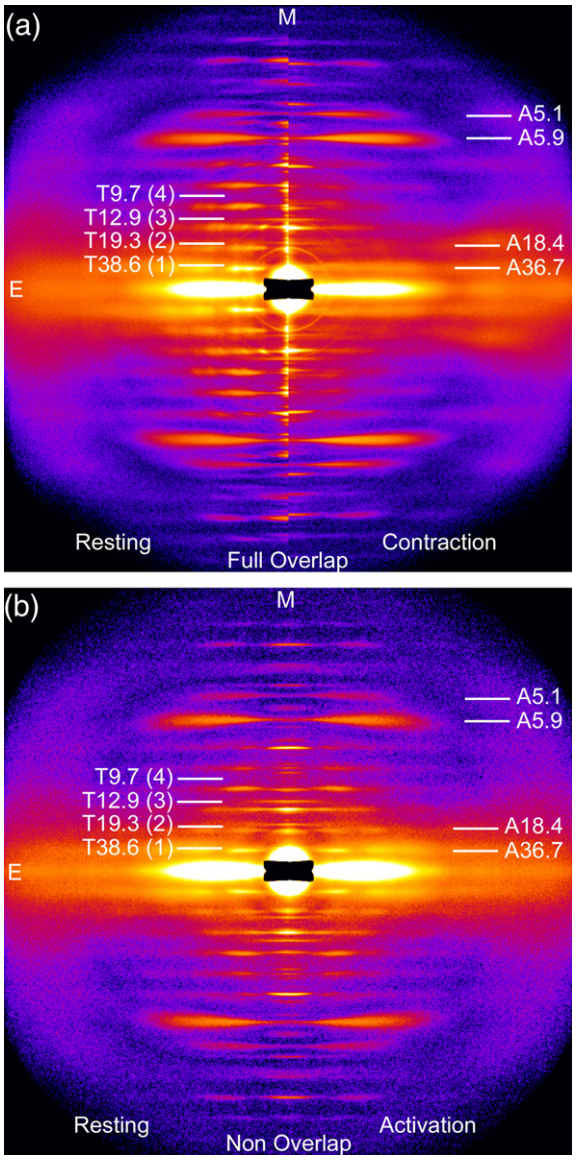

Fig. 1. X-ray diffraction patterns from live frog skeletal muscles. (a) A comparison between resting and contracting states of muscles at full filament overlap and (b) that between resting and activating states of overstretched muscles. The meridional axis (*M*) is coincided. The fiber axis is vertical. *E* is the equatorial axis. The letter T with a numerical value denotes the troponin-associated reflection with an axial spacing. The letter A, the actin-based reflections with the axial spacing.

initial peak decreased slightly ahead of the development of tension and it decreased to the level below the resting value (~45%) at the plateau of isometric tension. The intensity change of the TN1 reflection was consistent with the report by Maeda et al. [17]. However, the reflection width along the equator started to widen simultaneously with the development of tension. This change is caused by the partial loss of sampling effects due to the axial misalignment of the thin filaments in the hexagonal filament array, and the apparent intensity decrease with the development of tension was greatly suppressed to a value close to the resting level if we made the correction for an increase of a reflection width [17,24] (see Fig. 2C). The TN2 reflection apparently decreased in intensity without an appreciable initial rise below the rest level (~14%) at the plateau of tension, the intensity change running parallel to the development of tension. Its intensity change was also be affected by filament disordering. In contrast, the intensity of the TN3 reflection increased without an appreciable increase of the width, and when adjusted to a scale from 0 and 1, the change run ahead ($\tau_{1/2} \sim 38$ ms) of the development of tension ($\tau_{1/2} \sim 76$ ms) and it overshot the average level at the initial phase of tension plateau. In overstretched muscle, very small changes in intensity of TN2 and TN3 reflections were observed (also see Fig. 4A). Upon ceasing the stimulation, the intensities of three reflections returned toward their resting values, delayed substantially with respect to tension recovery. The TN1 intensity dropped simultaneously with the cessation of stimulation and returned gradually to the resting level. The time course of this intensity recovery closely paralleled the recovery of the reflection width (inset of Fig. 2C), suggesting that a slow recovery of TN reflections is correlated with the delayed restoration of the filament ordering. This behavior of the TN1 intensity was very similar to that of the 14.5-nm myosin-based meridional reflection [25]. However, the intensity drop after the cessation of stimulation did not accompany an appreciable change of the reflection width.

Intensity changes of the first and second thin filament-based layer lines

The first layer line components were separated from the nearby reflections in the high-angular resolution X-ray diffraction patterns, and their intensities in several radial regions were precisely measured. Fig. 3 shows the intensity changes in several radial regions during isometric contraction of muscle at full filament overlap (A) and those upon activation of overstretched muscles (B). The first layer line principal component (contributed by the J_2 Bessel function) denoted by an arrow (middle) in Fig. 3 decreased its intensity during isometric contraction, much greater than that occurring upon activation of overstretched muscles. While the intensity of the second layer line (contributed by the J_4 Bessel function) (2nd LL in Fig. 3) concomitantly increased during contraction, and the relative magnitude of its intensity increase was greater by about 3-fold than that upon activation of overstretched muscles. Thus the actin and myosin interaction causes the full intensity changes of the first and second layer lines. Such reciprocal intensity changes of these two principal low-angle layer lines indicate the enhancement of the 4-fold rotational symmetry of the thin filament which is greater in the force generating process than in the initial activation (see below).

Low-resolution modeling of structural changes of troponins in the thin filaments upon activation

Using the meridional intensities of the first four TN-associated reflections with the repeat of 38.4 nm measured

in the resting state and during the activation of overstretched muscles shown in Fig. 4A, one-dimensional modeling of the structure projected onto the fiber axis was performed to investigate the change of TNs bound to the thin filaments upon activation. We used a simple box function model (projected onto the fiber axis) of the TN molecule consisting of the globular core domain and the long tail domain in the lower diagram, which is based on the appearance of TN bound on the TM strand in electron micrographs [22] (Fig. 4B). The globular domain includes TNC, TNI and part of TNT (T2) and the tail domain includes the rest of TNT2 and TNT1. The model giving the lowest *R*-factor between the observed and calculated intensity data are shown for each state in Fig. 4C. The intensity of each TN-associated reflection calculated from the model with the lowest *R* value was compared with the observed one in Fig. 4A. In the resting state, the core domain and the tail domain of TN partially overlapped, and upon activation, the density of the core domain became greater than that in the resting state. Such a density change would be caused by orientational changes of the bridge-like V-shaped core domain of TN around and/or along the fiber axis, as suggested by FRET analysis [14], together with movements of TNT along the fiber axis. Modeling for contracting muscle at full filament overlap was not made because of undefined changes of the radial width of the reflections.

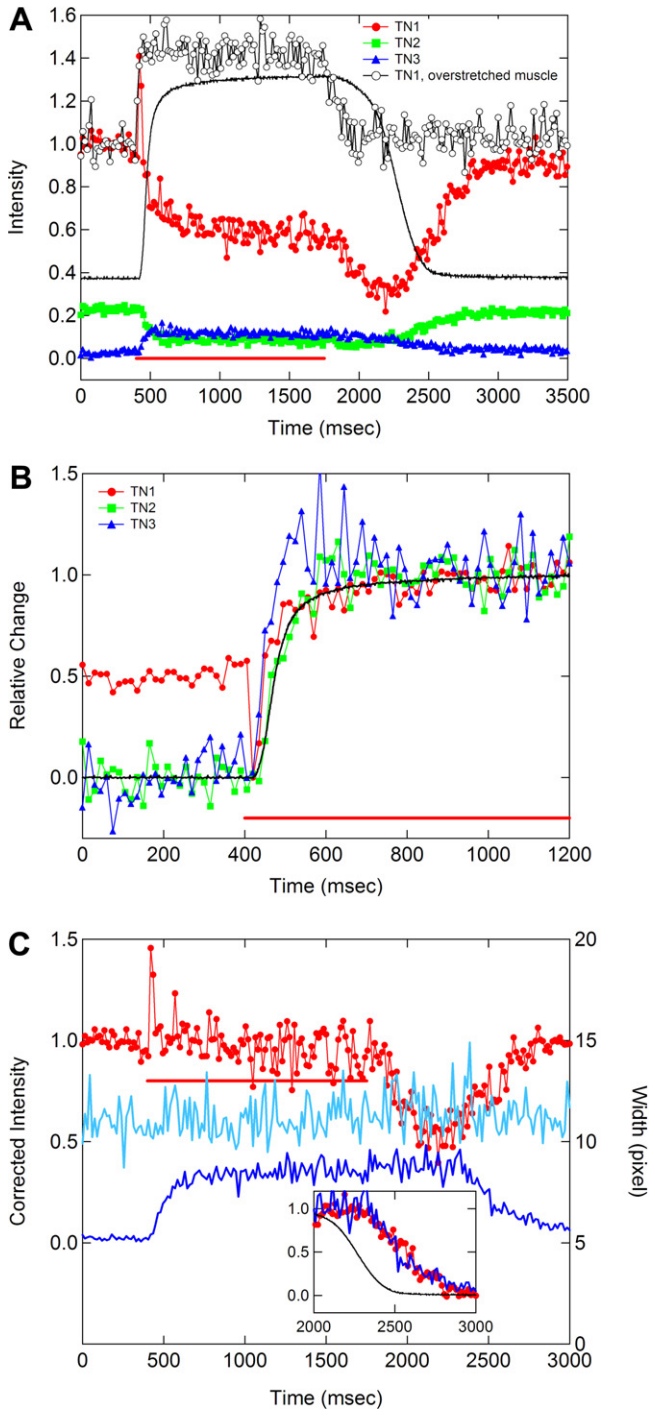

Fig. 2. (A) Time courses of the intensity changes of three troponin-associated meridional reflections from muscles at full filament overlap. The open circles denote the time course of the TN1 intensity change upon stimulation of overstretched muscles with the intensity level at rest coincident. (B) The 0–1 plot of the intensity changes of three TN reflections in (A). For the TN2 and TN3 reflections, the intensity levels at rest are defined as 0 and for the TN1 reflection, the value of the initial intensity drop just after stimulation is as 0. 1 is defined as the averaged intensity levels between 400 and 800 ms after the stimulation. (C) The time courses of the radial width of the TN1 reflection during isometric contraction of muscle at full filament overlap (dark blue), upon activation of overstretched muscle (light blue) and the intensities multiplied by the width changes (red). In the inset is shown the comparison of the time courses of the intensity change (red) and the width change (blue) during relaxation. In (A–C), the red horizontal bar denotes the period of the stimulation and the black curve, the tension change.

High-resolution modeling of structural changes of regulatory proteins in the thin filament during isometric contraction

Using the layer line intensities (up to $\sim$1/1.35 nm^{-1}) of the thin filament-based X-ray diffraction patterns in the resting state and during contraction, we have performed high-resolution modeling of the structural changes of the regulatory proteins in the thin filaments. We assumed that the intensity changes of these thin filament-based principal layer lines during contraction are ascribed solely to the structural changes occurring within the thin filaments by random attachments and asynchronous interactions with myosin heads [26]. In the modeling, the Holmes et al.'s model [23] was used as a starting model of F-actin, in which each of four subdomains of an actin monomer was further divided into four subgroups. The best-fit models were searched by moving all actin subgroups together with the regulatory proteins. The crystallographic shapes of the TM molecule and correctly weighted TN molecule (by the addition of the mass of the missing chains and TNT1 portion as a long helix) was approximated by space-filling with the spheres of 1.5-nm raisus. The structure of the arm part of TNI is

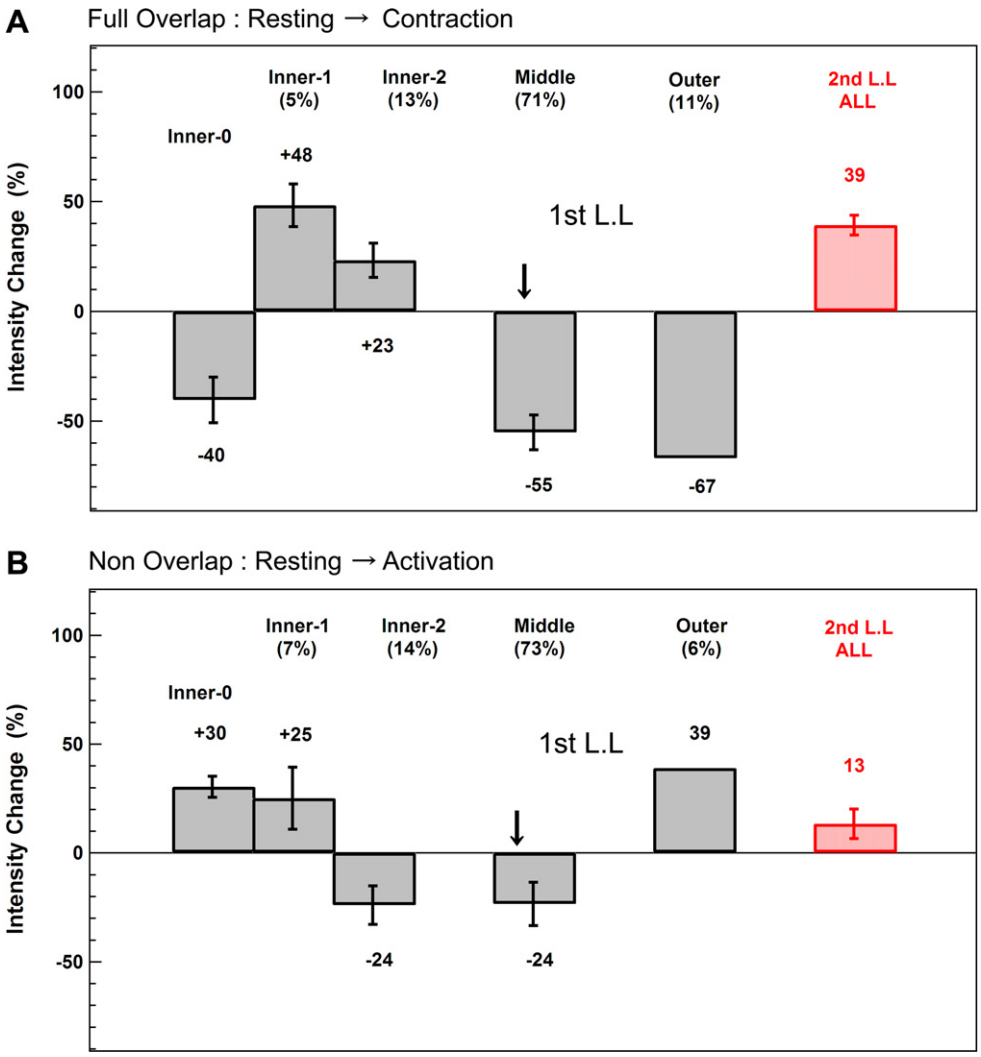

Fig. 3. The integrated intensities of the first (1st LL) and the second (2nd LL) thin filament-based layer lines during contraction of muscles at full filament overlap (A) and upon activation of overstretched muscles (B). The arrow indicates the "principal" part of the first layer line. Inner 0; TN component on the meridian, inner 1; TN component in the off-meridional portion, inner 2; TN + actin component, middle + outer; the first layer line principal component. The percentage denotes the intensity ratio of respective regions against the total layer line intensity. (From [18]).

unknown. We found plausible models for the disposition of the TN core domain region and the TM strands both in the resting and contracting states of muscles at full filament overlap which explained reasonably the observed layer line intensity data. The obtained models refined our previous models [18] and are depicted in Fig. 5A and B. The long axis of the TN core domain sitting at the radius of 5.37 nm was oriented nearly parallel to the TM strand in the resting state, and in the force generation state the core domain kept mostly its resting orientation but slewed around the filament axis with its center of gravity shifting slightly inward. The TNC moved by ~0.2 nm outward from the F-actin surface during contraction, consistent with the neutron scattering [11] and FRET data [14]. The long TNT1 part was located on the TM strand and moved together with the TM strand in the present modeling. In our studies, allowing TM and TNT1 to move independently did not yield good fits to the observed intensity data. The TM strands were located near subdomain 1 of actin at a radial position of about 3.43 nm from the filament axis in the resting state and moved toward the inner domain by ~20° in the contracting state with an increase of the radius by ~0.3 nm. In the models, the binding sites of myosin heads are covered by TM molecules in the resting state and uncovered during contraction. Preliminary modeling using the intensity data of overstretched muscle upon activation reveals that the TN core domain remained mostly in the resting position and the TM strand and TNT1 were located in an azimuthal position intermediate between the resting and contracting states, being possibly consistent with the docking model on the EM-reconstructed thin filament in the high Ca^{2+} state by Pirani et al. [13]. Our present modeling results concerning the TM shift do not support the implications of the FRET data [6]. More detailed modeling is needed to clarify this point. The calculated and observed layer line intensities are compared in Fig. 5C and D. The *R*-factor was ~0.14 in the

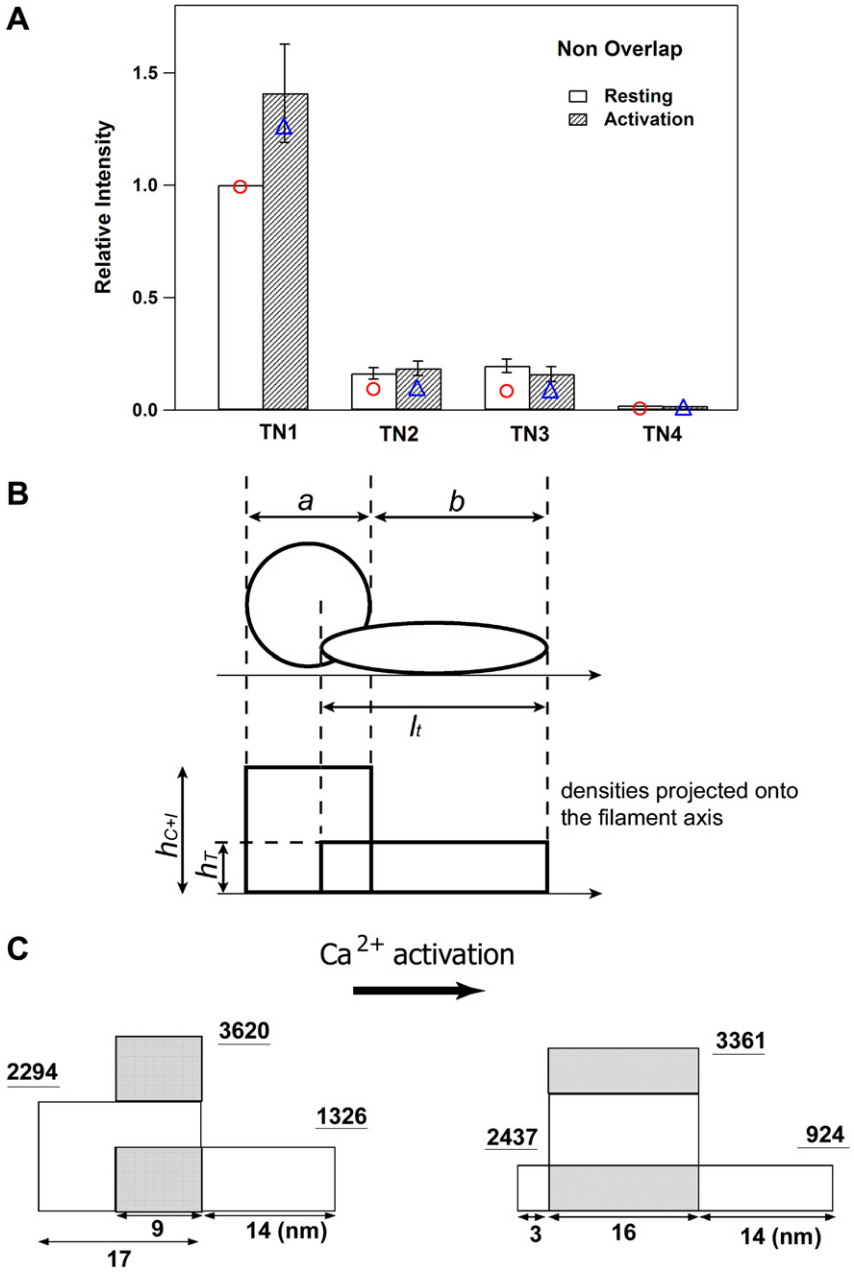

Fig. 4. (A) Intensity histograms of the first to fourth order TN-associated meridional reflections in the resting and activating states of overstretched muscles. The symbols on the bar graphs denote the calculated intensities from the respective models of the lowest *R*-value in (B). Vertical lines on bar graphs are associated SD. (B) The simplified model of TN bound to thin filaments and parameters used in the calculation. The circle and the flat ellipse denote the TN core domain and the TN tail domain, respectively (see text). The lower figure denotes the box functions mimicking the above model in which *a*, *b*, and *lt* denote the effective sizes of the core domain and the tail domain along the fiber axis, and h_{c+l} and h_T are the effective heights of the mass densities of the two domains projected onto the fiber axis. (C) The box function models giving the lowest *R*-value in each state of overstretched muscles. The gray box shows the mass portion of the overlap between two domains. The numerical values are the relative weights and the lengths of the respective parts. (Modified from [18]).

resting state and ~0.13 during contraction. Note that the outward shift of TNC within the core domain reproduce well the slight inner shifts of the intensity profiles of the 5.1- and 5.9-nm layer lines in the contracting state. The radial intensity profiles of the troponin-associated meridional reflections with the repeat of 38.4 nm calculated from the present models agreed well with data from the oriented sol of extracted thin filaments (T. Oda (RIKEN), unpublished data).

Spacing changes of troponin-associated meridional reflections

Spacing changes of the three TN-associated meridional reflections were investigated upon activation of overstretched muscles and during isometric contraction of muscles at full filament overlap. The average spacing changes of TN reflections relative to the resting values were compared with those of the actin-based reflections in Fig. 6A.

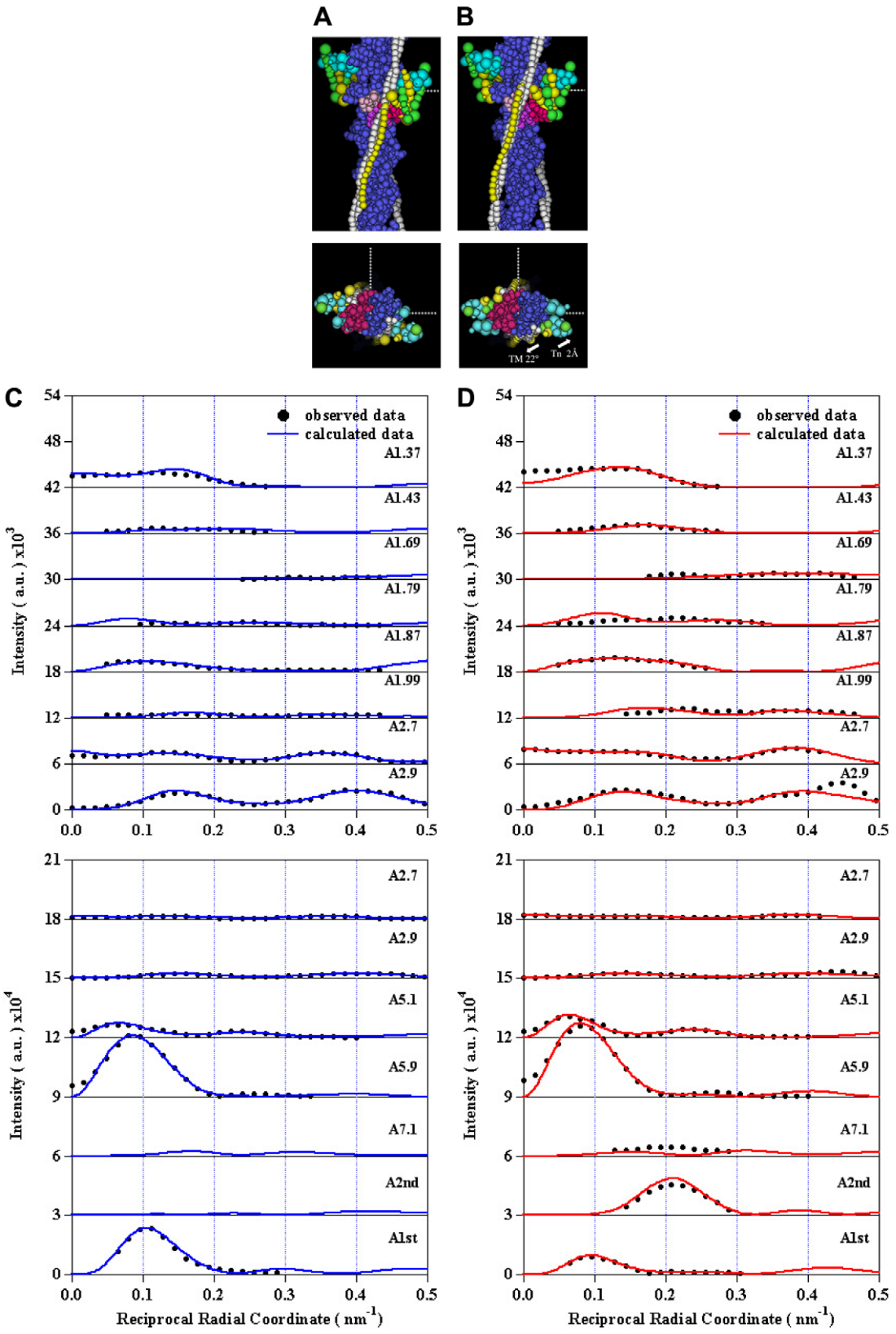

Fig. 5. The best-fit models of the thin filament in the resting state (A) and contracting states (B) with their cross-section viewed from the M-line. The upper side is toward the M-line in the side-views. F-actin is shown by blue balls, in which four main subdomains of an actin monomer are denoted by red, orange, magenta and pink in the order of the subdomain number. Tropomyosin (TM) is shown by the two strands of white balls and the troponin (TN) subunits are shown by light blue balls (TNC), green balls (TNI), and yellow balls (TNT). In the cross-section, the movements of TM and TNT in the transition of muscle from rest to isometric contraction were shown by arrows. In (C) and (D), the calculated and observed layer line intensities are compared.

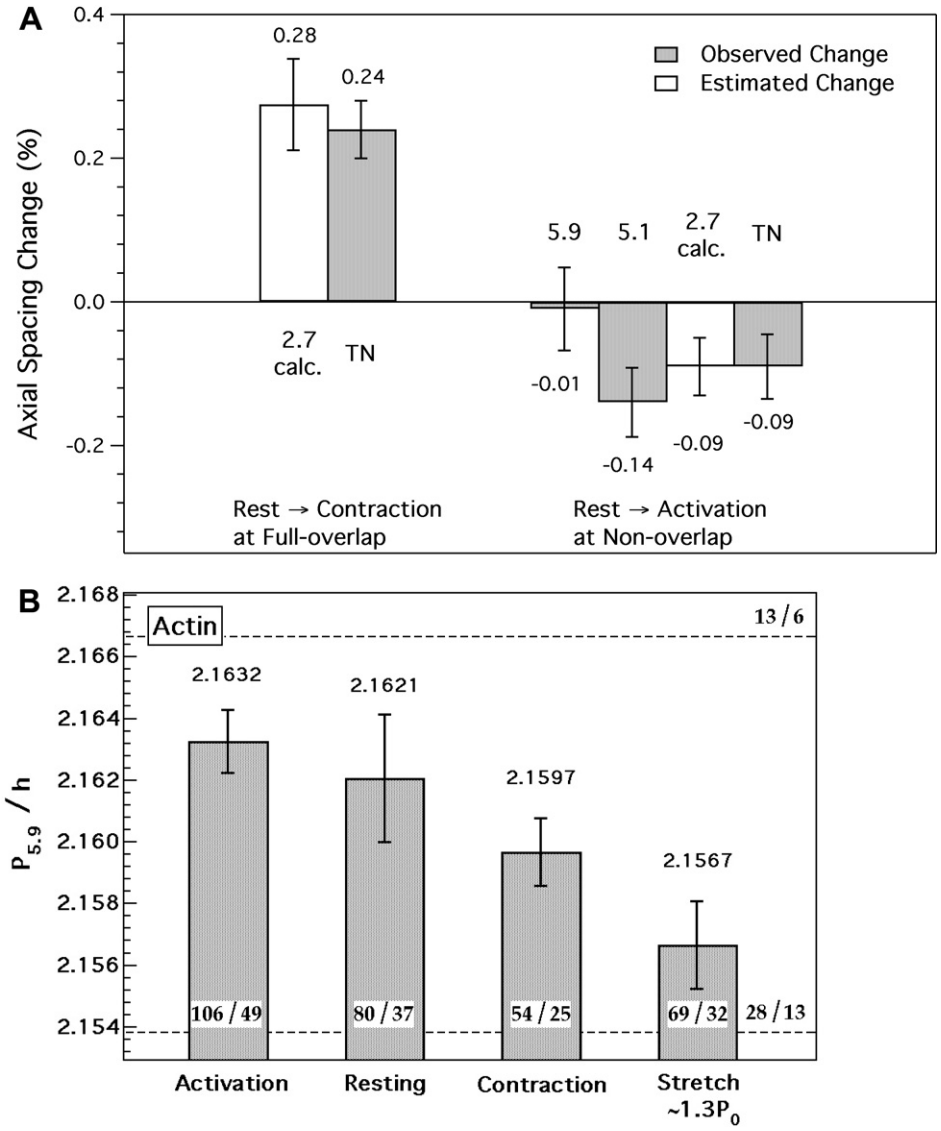

Fig. 6. (A) Fractional spacing changes of the TN-associated meridional reflections upon activation of overstretched muscles and during isometric contraction at full filament overlap. For a comparison, the spacing changes of three actin-based reflections are shown; 2.7, 5.1 and 5.9 denote the 2.7-nm meridional, 5.1- and 5.9-nm layer line reflections, respectively. The spacing change of the 2.7-nm reflection (2.7 calc.) was calculated from those of the 5.1- and 5.9-nm reflections. (B) The helical symmetry of the actin filament in various states of muscle. The helical symmetry expressed by residues/turns (the value within the bar-graph) was derived from the ratio (the value above the bar-graph) of the pitch of the 5.9-nm helix and the axial rise of the monomer in the filament. The two dashed lines denote the levels of the 13/6 symmetry and the 28/13 symmetry, respectively.

Upon activation of overstretched muscles, the average fractional spacing change decreased by ~0.09%. In the transition of muscles at full filament overlap from rest to isometric contraction, it increased by ~0.24%. Thus the activation and the actomyosin interaction caused the TN reflections to change spacing in opposite directions. These spacing changes of the TN-associated reflections followed those of the 2.7-nm actin meridional reflection, indicating that the repeating distance of TNs was altered by the extensibility of the actin filaments. As evidenced by the differential spacing changes of the actin reflections upon activation [27], the extensibility of the thin filaments was accompanied by the twisting change (twisting of right-handed helices). Thus, Ca^{2+}-binding to TN triggers the shortening and twisting changes of the actin filaments, possibly prerequisite for subsequent force generation. From the ratio of the axial spacings of the 5.9-nm layer line and the 2.7-nm meridional reflection, the helical symmetry of the actin filament can be estimated in various states (Fig. 6B). In the resting state, the ratio was 2.1621 and the actin filament has an 80 subunits/37 turns symmetry, and upon activation, it was 2.1632 and the actin helical symmetry shifts slightly toward the 13 subunits/6 turns symmetry (an 106/49 symmetry), representing a switch-on configuration of the thin actin filaments by Ca^{2+}-binding. (Note that this symmetry change upon activation differs in the direction from that derived from the electron micrographs of reconstituted thin filaments by addition of Ca^{2+} ions [28].) In

other word, the actin filament is strained in the resting state and Ca^{2+}-binding to TN would release the strain of actin filaments, leading to a stable equilibrium state. As the tension develops, it turns toward the 28 subunits/13 turns symmetry (a 54/25 symmetry), and this symmetry presumably yields an appropriate geometry for active interaction between actin and myosin crossbridges in their incommensurate periodicities.

Acknowledgments

We thank Drs. T. Kobayashi and K. Oshima for their kind help in X-ray experiments. Thanks are due to Dr. T.C. Irving for critical reading of the manuscript. This work was approved by the Photon Factory Advisory Committee (No. 01G370) and supported by Grant-in-Aid from the Ministry of Education, Science Sports and Culture of Japan (No. 13480220) (K.W.) and Grant from Special Coordination Funds from the Ministry of Education, Culture, Sports and Technology, Japan (K.W.).

References

[1] S. Ebashi, M. Endo, I. Ohtsuki, Control of muscle contraction, Quart. Rev. Biophys. 2 (1969) 351–384.
[2] V.L. Filatov, A.G. Katrukha, T.V. Bulargria, N.B. Gusev, Troponin: structure, properties, and mechanism of functioning, Biochemistry (Moscow) 64 (1999) 969–985.
[3] J.H. Brown, C. Cohen, Regulation of muscle contraction by tropomyosin and troponin: How structure illuminates function, Adv. Prot. Chem. 71 (2005) 121–159.
[4] W.T. Heller, E. Abusamhadneh, N. Finley, P.R. Rosevear, J. Trewhella, The solution structure of a cardiac troponin C–troponin I–troponin T complex shows a somewhat compact troponin C interacting with an extended troponin I–troponin T component, Biochemistry 41 (2002) 15654–15883.
[5] W.A. King, D.B. Stone, P.A. Timmins, T. Narayanan, A.A.M. von Brasch, R.A. Mendelson, P.M.G. Curmi, Solution structure of the chicken skeletal muscle troponin complex via small-angle neutron scattering and X-ray scattering, J. Mol. Biol. 345 (2005) 797–815.
[6] C. Kimura, K. Maeda, Y. Maeda, M. Miki, Ca2+ and S1-induced movement of troponin T on reconstituted skeletal muscle thin filaments observed by fluorescence energy transfer spectroscopy, J. Biochem. (Tokyo) 132 (2002) 93–102.
[7] A. Narita, T. Yasunaga, T. Ishikawa, K. Mayanagi, T. Wakabayashi, Ca^{2+}-induced switching of troponin and tropomyosin on actin filaments as revealed by electron cryo-microscopy, J. Mol. Biol. 308 (2001) 241–261.
[8] S. Takeda, A. Yamashita, K. Maeda, Y. Maeda, Structure of the core domain of human cardiac troponin in the Ca(2+)-saturated form, Nature 424 (2003) 35–41.
[9] M.V. Vinogradova, D.B. Stone, G.G. Malania, C. Karatzaferi, R. Cooke, R.A. Mendelson, R.J. Fletterick, Ca^{2+}-regulated structural changes in troponin, Proc. Natl. Acad. Sci. USA 102 (2005) 5038–5054.
[10] F. Matsumoto, K. Makino, K. Maeda, H. Patzelt, Y. Maeda, S. Fujiwara, Conformational changes of troponin C within the thin filaments detected by neutron scattering, J. Mol. Biol. 342 (2004) 1209–1221.
[11] S. Fujiwara, F. Matsumoto, Orientational information of troponin C within the thin filaments obtained by neutron fiber diffraction, J. Mol. Biol. 367 (2007) 16–24.
[12] K.J.V. Poole, M. Lorenz, G. Evans, G. Rosenbaum, A. Pirani, R. Craig, L.S. Tobacman, W. Lehman, K.C. Holmes, A comparison of muscle thin filament models obtained from electron microscopy reconstructions and low-angle X-ray fibre diagrams from non-overlap muscle, J. Struc. Biol. 155 (2006) 273–284.
[13] A. Pirani, M. Vinogradova, P.M.G. Curmi, W.A. King, R.J. Fletterick, R. Craig, L.S. Tobacman, C. Xu, V. Hatch, W. Lehman, J. Mol. Biol. 357 (2006) 707–717.
[14] C. Kimura-Sakiyama, Y. Ueno, K. Wakabayashi, M. Miki, Fluorescence resonance energy transfer between residues on troponin and tropomyosin in the reconstituted thin filament: modeling the troponin–tropomyosin complex, J. Mol. Biol. 376 (2008) 80–91.
[15] J. Bordas, G.P. Diakun, J.E. Harries, R.A. Lewis, G.R. Mant, M.L. Martin-Fernandez, E. Towns-Andrews, Two-dimensional time-resolved X-ray diffraction of muscle: Recent studies, Adv. Biophys. 27 (1991) 15–33.
[16] Y. Maeda, D. Popp, A. Stewart, Time-resolved X-ray diffraction study of the troponin-associated reflections from the frog muscle, Biophys. J. 63 (1992) 815–882.
[17] N. Yagi, An X-ray diffraction study on early structural changes in skeletal muscle contraction, Biophys. J. 84 (2003) 1093–1102.
[18] K. Wakabayashi, Y. Sugimoto, Y. Takezawa, Y. Ueno, S. Minakata, T. Matsuo, T. Kobayashi, Structural alterations of thin actin filaments in muscle contraction by synchrotron X-ray fibre diffraction, Adv. Exp. Med. Biol. 592 (2007) 327–340.
[19] N. Yagi, K. Inoue, T. Oka, CCD-based X-ray area detectors for time-resolved experiments, J. Synchrotron Radiat. 11 (2004) 456–461.
[20] Y. Amemiya, K. Wakabayashi, H. Tanaka, Y. Ueno, J. Miyahara, Laser-stimulated luminescence used to measure X-ray diffraction of a contracting striated muscle, Science 237 (1987) 164–168.
[21] K. Wakabayashi, Y. Sugimoto, H. Tanaka, Y. Ueno, Y. Takezawa, Y. Amemiya, X-ray diffraction evidence for the extensibility of actin and myosin filaments during muscle contraction, Biophys. J. 67 (1994) 2422–2435.
[22] P.F. Flicker, G.N. Phillips Jr., C. Cohen, Troponin and its interaction with tropomyosin. An electron microscopy study, J. Mol. Biol. 162 (1982) 495–501.
[23] K.C. Holmes, D. Popp, W. Gebhard, W. Kabsch, Atomic model of the actin filament, Nature 347 (1990) 44–49.
[24] Y. Sugimoto, Y. Takezawa, S. Minakata, T. Kobayashi, H. Tanaka, K. Wakabayashi, Time-resolved X-ray diffraction studies on skeletal muscle regulation: intensity changes of the troponin-associated meridional reflections during activation, Photon Factory Activity Rep. #20B (2003) 237.
[25] H.E. Huxley, A.R. Faruqi, M. Kress, J. Bordas, M.H.J. Koch, Time-resolved X-ray diffraction studies of the myosin layer-line reflections during muscle contraction, J. Mol. Biol. 158 (1982) 637–684.
[26] K. Wakabayashi, Y. Ueno, Y. Takezawa, Y. Sugimoto, Muscle contraction mechanism: use of X-ray synchrotron radiation, Encyclopedia of Life Sciences, Nature Publishing Group/www.els.net, (2001) 1–11.
[27] Y. Takezawa, Y. Sugimoto, K. Wakabayashi, Extensibility of actin and myosin filaments in various states of skeletal muscles as studied by X-ray diffraction, Adv. Exp. Med. Biol. 453 (1998) 309–317.
[28] J.M. Gillis, E.J. O'Brien, The effect of calcium ions on the structure of reconstituted muscle thin filaments, J. Mol. Biol. 99 (1975) 445–459.